Published in final edited form as:
Biomaterials. 2014 April ; 35(12): 3786–3793. doi:10.1016/j.biomaterials.2014.01.037.

The Influence of a Spatiotemporal 3D environment on Endothelial Cell Differentiation of Human Induced Pluripotent Stem Cells

Sophia Zhang[1], **James Dutton**[2], **Liping Su**[1], **Jianyi Zhang**[1,2,3], and **Lei Ye**[1,2]

[1]Division of Cardiology, Department of Medicine, University of Minnesota Medical School, Minneapolis, MN 55455, USA

[2]Stem Cell Institute, University of Minnesota Medical School, Minneapolis, MN 55455, USA

[3]Department of Biomedical Engineering, University of Minnesota, Minneapolis, MN 55455, USA

Abstract

Current EC differentiation protocols are inefficient, and the phenotypes of the differentiated ECs are only briefly stable, which significantly inhibits their utility for basic science research. Here, a remarkably more efficient hiPSC-EC differentiation protocol that incorporates a three-dimensional (3D) fibrin scaffold is presented. With this protocol, up to 45% of the differentiated hiPSCs assumed an EC phenotype, and after purification, greater than 95% of the cells displayed the EC phenotype (based on CD31 expression). The hiPSC-ECs continued to display EC characteristics for 4 weeks in vitro. Gene and protein expression levels of CD31, CD144 and von Willebrand factor-8 (vWF-8) were significantly up-regulated in differentiated hiPSC-ECs. hiPSC-ECs also have biological function to up-take Dil-conjugated acetylated LDL (Dil-ac-LDL) and form tubular structures on Matrigel. Collectively, these data demonstrate that a 3D differentiation protocol can efficiently generate ECs from hiPSCs and, furthermore, the differentiated hiPSC-ECs are functional and can maintain EC fate up to 4 weeks in vitro.

Keywords

Human induced pluripotent stem cells; Cell differentiation; scaffold

1. Introduction

The mechanisms that contribute to the transition from compensated heart disease to congestive heart failure (CHF) remain unclear but may be related to increases in wall stress, which can induce metabolic abnormalities and progressive contractile dysfunction in the region of viable myocardium that surrounds the infarct (i.e., the border zone, [BZ]) [1, 2]. Although transplanted cardiac progenitor cells can repair damaged myocardium to some extent [3, 4], the improvement is believed to evolve primarily through the induction of

Corresponding author: Lei Ye Assistant Professor of Medicine Department of Medicine University of Minnesota MN, 55455 USA ylei@umn.edu.

CONFLICT OF INTERESTS: NA

paracrine mechanisms, because the engraftment rate of the transplanted cells is low, and the differentiation of engrafted cells into functional cardiomyocytes (CMs) occurs even less frequently [5-8]. It is hypothesized that these limitations can be circumvented by placing a patch of differentiated CMs and endothelial cells (ECs) over the site of infarction, and that the cell patch can prevent left ventricular (LV) scar bulging, reduce wall stress, improve myocardial bioenergetics, and limit contractile dysfunction in the BZ [5, 8, 9]. Human cardiac muscle patches can be created by differentiating human induced pluripotent stem cells (hiPSC) into CMs, smooth-muscle cells (SMCs), and endothelial cells (ECs) and then entrapping the differentiated cells in a three-dimensional (3D), porous, fibrin scaffold, which can be designed to simulate the microenvironment of the myocardium.

The current protocols for differentiating human pluripotent stem cells into ECs are unsatisfactory because the yield is low (typically less than 15%) [10-12] and the characteristic EC phenotype is usually maintained for only 14 days or less [10, 11]. ECs are known to play extremely important roles in cardiovascular physiology [13, 14], by mediating vital signaling pathways that regulate myocardial vascularization, perfusion, metabolism, and contractile performance [13, 14]. Previously, the lack of quality EC lines derived from pluripotent stem cells represented a significant obstacle for the field of cardiovascular science. The pluripotent stem cell differentiation during the embryonic development phase of the vertebrate heart is a complicated process. This process involves cell proliferation, migration, rearrangement and differentiation, which are all regulated by the spatiotemporal changes of signaling pathways within the extracellular matrix (ECM). Although not much is known about the ECM spatiotemporal signaling pathways that regulate embryonic development, it is evident that the traditional 2D cell culture systems lack the major component of the 3D environment that pluripotent stem cells are exposed to in the nature. For the studies reported here, it is hypothesized that the hiPSC-EC phenotype requires 3D surface tension, and consequently the differentiation of hiPSCs into ECs should be improved by suspending the cells in a 3D biomaterial matrix entrapping the respective EC inducers. A 3D porous fibrin was chosen as the scaffold, which enabled control over the binding of needed peptides and the timing of degradation of the matrix [15]. These experiments used two established hiPSC lines, PCBC16iPS and GRiPS. The efficiency of this 3D differentiation protocol was evaluated with analysis flow cytometry and immunohistochemistry.

2. Methods

2.1 Culture of hiPSCs

The PCBC16iPS and GRiPS cell lines were created by using the non-integrating Sendai virus to transfect neonatal human dermal fibroblasts (Lonza, USA) with the reprogramming factors OCT4, SOX2, KLF4, and C-MYC, as described previously [16]. The GRiPS cell line was also engineered to express green fluorescent protein (GFP).

2.2 Differentiation of hiPSCs into endothelial cells

The differentiation protocol was outlined in Figure 1A. Briefly, two to three days before initiating differentiation, hiPSCs were dissociated into single cells; then, cells in the control group were seeded as a monolayer into 6-well plates with mTeSR1 medium, and cells in the scaffold group were seeded into a 0.5-mL fibrin scaffold patch on a 24-well plate and transferred to 6-well plates. The first stage of differentiation was initiated (on day 0) by culturing the cell-containing fibrin scaffold in EBM2 medium (Lonza USA) supplemented with B27 without insulin, activin-A, and bone morphogenetic protein 4 **(**BMP4) for 24 hours. Stage 2 was initiated on day 1 by replacing the medium with EBM2 medium supplemented with B27 without insulin, vascular endothelial growth factor (VEGF),

erythropoietin (EPO), and transforming growth factor β1 (TGFβ1), and then culturing the cells for 48 hours; the medium was refreshed on day 3, and the cells were cultured for another 48 hours. On day 5, the differentiating hiPSCs were released by treating the patch with collagenase IV, and the medium was replaced with EGM2-MV medium (Lonza, USA) supplemented with B27, VEGF, and SB-431542. The medium was changed every 2 days, and differentiation efficiency was evaluated on day 14 via fluorescence activated cell sorting (FACS); cells positive for CD31 expression and for both CD31 and CD144 expression were collected and expanded. The purified hiPSC-ECs were cultured in EGM2-MV medium supplemented with B27, VEGF, and SB-431542. The cell culture medium was changed every two days.

2.3 Immunohistochemistry

Differentiated hiPSC-ECs were fixed with 4% paraformaldehyde for 20 minutes at room temperature, permeabilized in 0.1% Triton X-100 at 4°C for 10 minutes, and then blocked with UltraV block (Fisher Scientific, USA) for 7 minutes. Primary antibodies (monoclonal anti-CD31 and mouse anti-CD144 [BD Pharmingen, USA]; goat anti-vWF [Santa Cruz Biotechnology, USA]) at a concentration of 1:100 were added to the UltraV block buffer and incubated overnight at 4°C; then, the cells were incubated with FITC-or TRITC-conjugated secondary antibodies (donkey anti-mouse or goat IgG) in UltraV block buffer for 1 hour at room temperature, labeled with DAPI, washed, and viewed under a fluorescence microscope (Olympus, Japan).

2.4 Flow Cytometry

Differentiated hiPSC-ECs were trypsinized and re-suspended as single cells in glass tubes, incubated with UltraV block for 7 minutes at room temperature, and then incubated with 2% fetal bovine serum (FBS) in phosphate-buffered saline (PBS) containing primary PE- or APC-conjugated anti-CD31 antibodies and PE-conjugated anti-CD144 antibodies, or isotype control antibodies (BD Pharmingen, USA) for 30 min at 4°C. The cells were washed with 2% FBS/PBS, re-suspended in 0.3 mL 2% FBS/PBS containing 5 μL of propidium iodide (10 μg/mL), and evaluated with a FACS Aria instrument (BD Biosciences, USA). Cells of adequate size and granularity were used for statistical analysis [17].

2.5 hiPSC-EC functional studies

The biological function of hiPSC-ECs was assessed via Dil-conjugated acetylated low-density lipoprotein (Dil-ac-LDL) uptake and tube formation. For the Dil-ac-LDL uptake assay, hiPSC-ECs were incubated with 10 μg/mL of Dil-Ac-LDL (Life Technologies, USA) at 37°C for 6 hours, washed with Dulbecco's PB S, fixed, and counterstained with DAPI. For the tube-formation assay, cells were seeded in 48-well plates that had been coated with Matrigel (BD Pharmingen, USA) and incubated at 37°for 12 hours.

2.6 Quantitative RT-PCR (QRT-PCR) analysis

Undifferentiated hiPSCs and purified hiPSC-ECs on day-1 were collected to quantify the expression of CD31, CD144, and vWF-8. The primers used for CD31 were TTGAGACCAGCCTGATGAAACCCT (forward) and TCCGTTTCCTGGGTTCAAGCGATA (reverse); CD144 were TGTGGGCTCTCTGTTTGTTGAGGA (forward) and TGGCCTCGACGATGAAGCTGTATT (reverse); and vWF-8 were AGGTGAATGTGAAGAGGCCCATGA (forward) and CTTTGCCCAGCAGCAGAATGATGT (reverse). GAPDH was used as an internal control [16]. Total RNA was isolated and cDNA was synthesized as described earlier [16, 18]. The QPCR thermal cycling program comprised 40 cycles, and each cycle consisted of enzyme

activation at 95°C for 15 minutes, denaturation at 95°C for 30 seconds, annealing at 60°C for 30 seconds, and extension at 72°C for 30 seconds. The gene expression levels of CD31, CD144, and vWF-8 mRNA were normalized to GAPDH, and presented as fold changes [16].

2.7 Statistics

Statistical analyses were performed with SPSS software (version 20.0). All data is presented as mean ± standard deviation (SD).

3. Results

3.1 Differentiation of EC from hiPSC

hiPSCs were cultured as either a monolayer of cells or after suspending them in a 3D fibrin scaffold. The hiPSC-containing scaffolds formed a circular patch of 15-mm diameter (Figure 1B), and within the scaffold, the hiPSCs self-assembled into small clusters (Figure 1C) that grew into spheres 2 days later (Figure 1D). During the first stage of the differentiation protocol, hiPSCs were committed to the mesodermal lineage by culturing them with activin A and BMP-4 for 24 hours [16]. In stage 2, the cells were cultured in VEGF, TGFβ1, and EPO for 96 hours. Small spheres of hiPSCs were observed at the end of stage 1 (i.e., on Day 1) (Figure 1E), and the spheres formed spike-like structures after stage 2 (i.e., on Day 5) (Figure 1F). When the differentiated cells were released by treating the scaffold with collagenase IV, they adhered to the surface of the culture dish and formed a single layer of cells (Figure 1G).

3.2 3D fibrin scaffold enhanced hiPSC-ECs differentiation efficiency

The efficiencies of the monolayer- and patch-mediated differentiation protocols were evaluated 14 days after differentiation was initiated by performing flow cytometry analyses for CD31 expression. Only 4.2±1.4% of GRiPS and 5.1±2.7% of PCBC16iPS (Figure 2A, B) cells expressed CD31 when the cells were cultured in a monolayer. However, the EC differentiation efficiency increased to 43.8±0.9% (maximum: 45.5%; minimum: 40.8%) for GRiPS (Figure 2C), and 26.8±5.2% (maximum: 31.2%; minimum: 21%) for PCBC16iPS (Figure 2D) when the cells were cultured in the 3D porous fibrin scaffold (Figure 2).

3.3 Maintenance of the EC phenotype

The hiPSC-ECs were purified to >95% CD31+ cells via flow cytometry and then cultured in EGM2-MV medium (without FBS) supplemented with B27, VEGF, and SB431542. The durability of the EC phenotype was evaluated by performing flow cytometry analyses for CD31 and CD144 expression at 2, 3, and 4 weeks after purification (Figure 3A-C); each marker was expressed by >90% of the hiPSC-ECs at all three time points (Figure 3D).

3.4 Characterization of hiPSC-ECs

The purified hiPSC-ECs grew to form a cobblestone-like monolayer on culture plates (Figure 4A&B), and levels of CD31, CD144, and vWF-8 mRNA were more than 1000-fold greater in purified hiPSC-ECs than in undifferentiated hiPSCs (Figure 4C). Robust evidence of CD31, CD144, and vWF-8 protein expression was also observed (Figure 4D-F), and the cells were positive for Dil-ac-LDL uptake and for tube formation on Matrigel, at Week 1 and Week 4 after purification (Figure 4G&H).

4. DISCUSSION

The findings presented in this report show that 1) the efficiency of hiPSC-EC differentiation can be markedly increased (to ~45%) by seeding the cells into a 3D fibrin scaffold and 2) that ~90% of the ECs obtained via this protocol continue to display EC characteristics for at least 4 weeks in vitro, which is approximately twice as long as previously observed [11]. The findings support a concept that the effectiveness of the hiPSC-EC differentiation protocol requires the physical 3D surface tension induced by the scaffold, which may entrap the inducers and mimic the microenvironment of developing myocardium.

The success in making induced pluripotent stem cells (iPSCs) offers additional advantages in providing immunologically compatible autologous hiPSCs and enabling potential "personalized" therapy in the future. Effective protocols for differentiating hiPSCs into SMCs [19] and CMs [20] have recently been introduced, but the two most common methods for deriving ECs from hiPSCs, embryoid-body (EB) formation [11, 12] and co-culturing with murine stromal cells [10, 19], are unsatisfactory. The embryoid-body method is inefficient and produces unstable cells (<15% of the cells assume an EC phenotype, and the phenotype is maintained for ≤14 days), while the co-culturing method can leave a small number of murine lineage cells in the hiPSC-EC population [10, 19].

The data from the present study demonstrate that the efficiency of ECs-hiPSC differentiation and quality of derived ECs-hiPSC were significantly improved when hiPSCs were cultured in the 3D environment. These findings support a concept that the effectiveness of the hiPSC-EC differentiation protocol requires the physical 3D surface tension induced by the scaffold, which may entrap the inducers and mimic the microenvironment of developing myocardium. In the present study, the specific combination of factors and timing used in the protocol also contributed significantly to the improvement of differentiation efficiency of the hiPSC –ECs (Figures 1-4). During *in vivo* embryonic development, fate specification of stem cells is regulated by the cell microenvironments, in which a variety of biochemical and biophysical signals are presented within the 3D extracellular matrices. Future studies are warranted to decipher the mechanisms of these spatiotemporal factors.

It is known that the extracellular microenvironment is critically important for cell growth, differentiation and morphogenesis [21-23]. Several studies have shown that the activity and differentiation of stem/progenitor cells can be altered by mechanical stress. For example, cyclic mechanical loading can enhance the differentiation of human mesenchymal stem cells (MSCs) into osteoblast-like cells [22], and agarose or collagen has been used to induce a compressive force on cultured MSCs, which subsequently promoted chondrogenesis by increasing the production of type II collagen, aggrecan, and chondrogenic-specific transcription factors [21]. Mechanical strain has also been used to increase the expression of osteogenic markers such as cbfa-1, osteopontin, osteocalcin, and TGFβ1 by osteoblast precursor cells in a collagen matrix [23]. However, these previous investigations have been limited to cells that are involved in bone or cartilage regeneration. Surprisingly, few studies in the literature have applied mechanical force in differentiation of ECs from pluripotent stem cells. Thus, the results presented here are among the first to suggest that physical strain may have a crucial role in the differentiation of ECs. We believe that the fibrin scaffold used in our protocol promotes the differentiation of hiPSCs into ECs by mimicking the 3D tension that is present in the microenvironment of the developing endothelium. The mechanisms that link mechanical tension to EC differentiation have yet to be characterized but may involve the activation of phosphatidylinositol 3-kinase (PI3K) and its downstream effector PECAM-1 (CD31) [24], which is a key endothelial mechanosensor that influences both the physiological and pathological development of blood vessels [25, 26].

The effectiveness of our hiPSC-EC differentiation protocol can also be attributed to the specific regimen of factors added to the culture medium. The factors used in stage 1, activin-A and BMP-4, are known to commit hiPSCs to the mesodermal lineage [16], while the stage-2 factors VEGF [27] and TGFβ1 [28] have been linked to the differentiation of embryonic stem cells (ESCs) or ESC-derived cells into ECs, and EPO regulates the differentiation and proliferation of endothelial progenitor cells [29]. However, the batch variability of FBS can adversely affect the fate of hiPSC-ECs, and TGFβ1 limits EC proliferation [30]. So the purified hiPSC-ECs were maintained in B27 serum with VEGF and SB-431542, which inhibits the kinase activity of TGF-β receptors and facilitates the proliferation of hiPSC-ECs [31]. Furthermore, the fibrin scaffold can be modified to bind and release many of the factors that regulate EC differentiation, proliferation, and maturation; thus, as future studies characterize the spatiotemporal interactions among these factors, our protocol can continue to be optimized by incorporating this new knowledge into the scaffold's design.

5. Conclusion

We have developed a protocol for generating ECs from hiPSCs that is remarkably more efficient and robust than conventional methods and avoids the risk of xenogenic or allogenic contamination. Up to 45% of the differentiated hiPSCs assumed an EC phenotype, and after purification, ~90% of the hiPSC-ECs continued to display EC characteristics for 4 weeks in vitro, which is ~2 weeks longer than has been observed for conventionally prepared hiPSC-ECs. The efficiency of this differentiation protocol and durability of the hiPSC-EC phenotype have obvious and beneficial implications for their potential use in the clinic or as a platform for drug testing, and for the development of new cardiovascular tissue engineering technologies.

Acknowledgments

This work was supported by US Public Health Service grants NIH RO1 HL67828, HL95077, HL114120, and UO1HL100407. The authors would like to thank Mr. W. Kevin Meisner for his editorial assistance.

REFERENCES

1. Bolognese L, Neskovic AN, Parodi G, Cerisano G, Buonamici P, Santoro GM, et al. Left ventricular remodeling after primary coronary angioplasty: patterns of left ventricular dilation and long-term prognostic implications. Circulation. 2002; 106:2351–7. [PubMed: 12403666]
2. Hu Q, Wang X, Lee J, Mansoor A, Liu J, Zeng L, et al. Profound bioenergetic abnormalities in peri-infarct myocardial regions. Am J Physiol Heart Circ Physiol. 2006; 291:H648–57. [PubMed: 16582014]
3. Hatzistergos KE, Quevedo H, Oskouei BN, Hu Q, Feigenbaum GS, Margitich IS, et al. Bone marrow mesenchymal stem cells stimulate cardiac stem cell proliferation and differentiation. Circ Res. 2010; 107:913–22. [PubMed: 20671238]
4. Leri A, Kajstura J, Anversa P. Role of cardiac stem cells in cardiac pathophysiology: a paradigm shift in human myocardial biology. Circ Res. 2011; 109:941–61. [PubMed: 21960726]
5. Wang X, Hu Q, Nakamura Y, Lee J, Zhang G, From AH, et al. The role of the sca-1+/CD31- cardiac progenitor cell population in postinfarction left ventricular remodeling. Stem Cells. 2006; 24:1779–88. [PubMed: 16614004]
6. Wang X, Jameel MN, Li Q, Mansoor A, Qiang X, Swingen C, et al. Stem cells for myocardial repair with use of a transarterial catheter. Circulation. 2009; 120:S238–46. [PubMed: 19752374]
7. Xiong Q, Hill KL, Li Q, Suntharalingam P, Mansoor A, Wang X, et al. A fibrin patch-based enhanced delivery of human embryonic stem cell-derived vascular cell transplantation in a porcine model of postinfarction left ventricular remodeling. Stem Cells. 2011; 29:367–75. [PubMed: 21732493]

8. Xiong Q, Ye L, Zhang P, Lepley M, Swingen C, Zhang L, et al. Bioenergetic and functional consequences of cellular therapy: activation of endogenous cardiovascular progenitor cells. Circ Res. 2012; 111:455–68. [PubMed: 22723295]
9. Zeng L, Hu Q, Wang X, Mansoor A, Lee J, Feygin J, et al. Bioenergetic and functional consequences of bone marrow-derived multipotent progenitor cell transplantation in hearts with postinfarction left ventricular remodeling. Circulation. 2007; 115:1866–75. [PubMed: 17389266]
10. Choi KD, Yu J, Smuga-Otto K, Salvagiotto G, Rehrauer W, Vodyanik M, et al. Hematopoietic and endothelial differentiation of human induced pluripotent stem cells. Stem Cells. 2009; 27:559–67. [PubMed: 19259936]
11. Li Z, Hu S, Ghosh Z, Han Z, Wu JC. Functional characterization and expression profiling of human induced pluripotent stem cell- and embryonic stem cell-derived endothelial cells. Stem Cells Dev. 2011; 20:1701–10. [PubMed: 21235328]
12. Rufaihah AJ, Huang NF, Jame S, Lee JC, Nguyen HN, Byers B, et al. Endothelial cells derived from human iPSCS increase capillary density and improve perfusion in a mouse model of peripheral arterial disease. Arterioscler Thromb Vasc Biol. 2011; 31:e72–9. [PubMed: 21836062]
13. Brutsaert DL. Cardiac endothelial-myocardial signaling: its role in cardiac growth, contractile performance, and rhythmicity. Physiol Rev. 2003; 83:59–115. [PubMed: 12506127]
14. Hsieh PC, Davis ME, Lisowski LK, Lee RT. Endothelial-cardiomyocyte interactions in cardiac development and repair. Annu Rev Physiol. 2006; 68:51–66. [PubMed: 16460266]
15. Liu J, Hu Q, Wang Z, Xu C, Wang X, Gong G, et al. Autologous stem cell transplantation for myocardial repair. Am J Physiol Heart Circ Physiol. 2004; 287:H501–11. [PubMed: 15277194]
16. Ye L, Zhang S, Greder L, Dutton J, Keirstead SA, Lepley M, et al. Effective cardiac myocyte differentiation of human induced pluripotent stem cells requires VEGF. PloS One. 2013; 8:e53764. [PubMed: 23326500]
17. Ye L, Haider H, Esa WB, Law PK, Zhang W, Su L, et al. Nonviral vector-based gene transfection of primary human skeletal myoblasts. Exp Biol Med (Maywood). 2007; 232:1477–87. [PubMed: 18040073]
18. Ye L, Zhang W, Su LP, Haider HK, Poh KK, Galupo MJ, et al. Nanoparticle based delivery of hypoxia-regulated VEGF transgene system combined with myoblast engraftment for myocardial repair. Biomaterials. 2011; 32:2424–31. [PubMed: 21216458]
19. Woll PS, Morris JK, Painschab MS, Marcus RK, Kohn AD, Biechele TL, et al. Wnt signaling promotes hematoendothelial cell development from human embryonic stem cells. Blood. 2008; 111:122–31. [PubMed: 17875805]
20. Zhang J, Klos M, Wilson GF, Herman AM, Lian X, Raval KK, et al. Extracellular matrix promotes highly efficient cardiac differentiation of human pluripotent stem cells: the matrix sandwich method. Circ Res. 2012; 111:1125–36. [PubMed: 22912385]
21. Takahashi I, Nuckolls GH, Takahashi K, Tanaka O, Semba I, Dashner R, et al. Compressive force promotes sox9, type II collagen and aggrecan and inhibits IL-1beta expression resulting in chondrogenesis in mouse embryonic limb bud mesenchymal cells. J Cell Sci. 1998; 111:2067–76. Pt 14. [PubMed: 9645953]
22. Kang MN, Yoon HH, Seo YK, Park JK. Effect of mechanical stimulation on the differentiation of cord stem cells. Connect Tissue Res. 2012; 53:149–59. [PubMed: 22149641]
23. Ignatius A, Blessing H, Liedert A, Schmidt C, Neidlinger-Wilke C, Kaspar D, et al. Tissue engineering of bone: effects of mechanical strain on osteoblastic cells in type I collagen matrices. Biomaterials. 2005; 26:311–8. [PubMed: 15262473]
24. Collins C, Guilluy C, Welch C, O'Brien ET, Hahn K, Superfine R, et al. Localized tensional forces on PECAM-1 elicit a global mechanotransduction response via the integrin-RhoA pathway. Curr Biol. 2012; 22:2087–94. [PubMed: 23084990]
25. Tzima E, Irani-Tehrani M, Kiosses WB, Dejana E, Schultz DA, Engelhardt B, et al. A mechanosensory complex that mediates the endothelial cell response to fluid shear stress. Nature. 2005; 437:426–31. [PubMed: 16163360]
26. Harry BL, Sanders JM, Feaver RE, Lansey M, Deem TL, Zarbock A, et al. Endothelial cell PECAM-1 promotes atherosclerotic lesions in areas of disturbed flow in ApoE-deficient mice. Arterioscler Thromb Vasc Biol. 2008; 28:2003–8. [PubMed: 18688018]

27. Yamashita J, Itoh H, Hirashima M, Ogawa M, Nishikawa S, Yurugi T, et al. Flk1-positive cells derived from embryonic stem cells serve as vascular progenitors. Nature. 2000; 408:92–6. [PubMed: 11081514]

28. Gualandris A, Annes JP, Arese M, Noguera I, Jurukovski V, Rifkin DB. The latent transforming growth factor-beta-binding protein-1 promotes in vitro differentiation of embryonic stem cells into endothelium. Mol Biol Cell. 2000; 11:4295–308. [PubMed: 11102524]

29. Bahlmann FH, DeGroot K, Duckert T, Niemczyk E, Bahlmann E, Boehm SM, et al. Endothelial progenitor cell proliferation and differentiation is regulated by erythropoietin. Kidney Int. 2003; 64:1648–52. [PubMed: 14531796]

30. Beck L Jr. D'Amore PA. Vascular development: cellular and molecular regulation. FASEB J. 1997; 11:365–73. [PubMed: 9141503]

31. Watabe T, Nishihara A, Mishima K, Yamashita J, Shimizu K, Miyazawa K, et al. TGF-beta receptor kinase inhibitor enhances growth and integrity of embryonic stem cell-derived endothelial cells. J Cell Biol. 2003; 163:1303–11. [PubMed: 14676305]

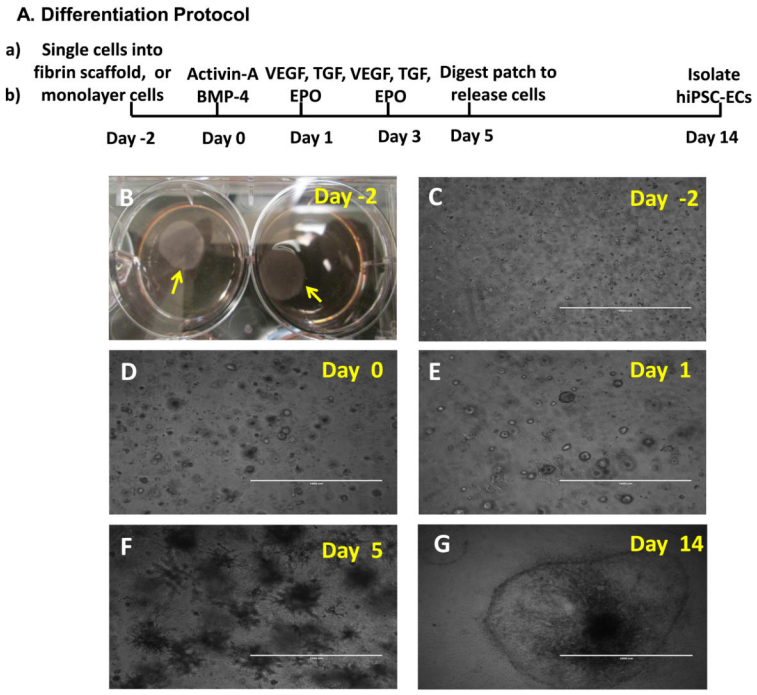

Figure 1. 3D scaffold-mediated differentiation of hiPSCs into hiPSC-ECs

(A) A schematic diagram of the hiPSC-EC differentiation protocol is displayed. **(B)** Two days before the differentiation protocol was initiated (i.e., on Day -2), fibrinogen solution was loaded with hiPSCs and mixed with thrombin to form a hiPSC-containing scaffold (yellow arrow). **(C)** The cells self-assembled into small clusters within the patch and grew to form sphere-shaped structures on **(D)** Day 0, when stage 1 of differentiation was initiated by culturing the cells with activin A and BMP-4. **(E)** On Day 1 (i.e., 24 hours later), stage 2 of differentiation was initiated by replacing the activin A/BMP-4 medium with medium containing VEGF, EPO, and TGFβ1, and the cells were cultured for 96 hours (i.e., until Day 5). **(F)** After 5 days of differentiation, the spheres had grown into spike-like structures, which were released from the patch via collagenase IV digestion. **(G)** By Day 14, the differentiated hiPSCs (visible as a sphere attached to the cell culture surface and formed a single layer of cells. (C-F: Bar=1 mm; G: Bar=2 mm).

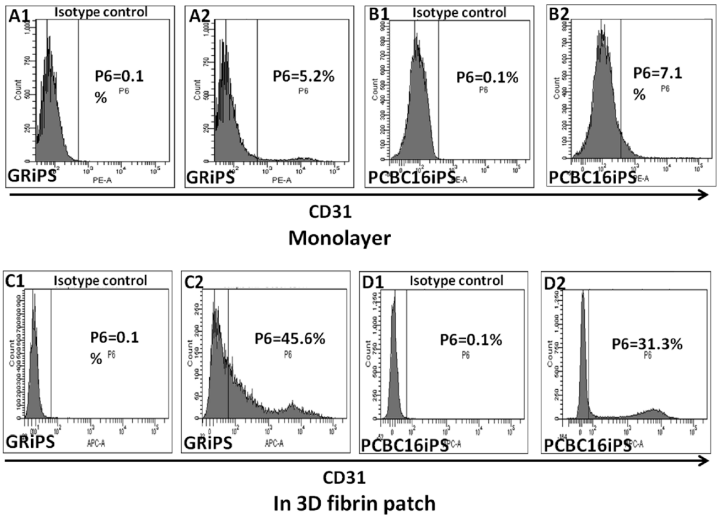

Figure 2. The efficiency of hiPSC-EC differentiation increases when the cells are encapsulated in a fibrin patch

hiPSCs were differentiated **(A1-B2)** in monolayers or **(C1-D2)** after suspension in a fibrin patch. Differentiation efficiency was evaluated by comparing **(A2, B2, C2, D2)** CD31 expression with isotype controls **(A1, B1, C1, D1)** via flow cytometry. The maximum efficiencies obtained with each differentiation protocol are shown for both GRiPS- and PCBC16iPS-lineage cells.

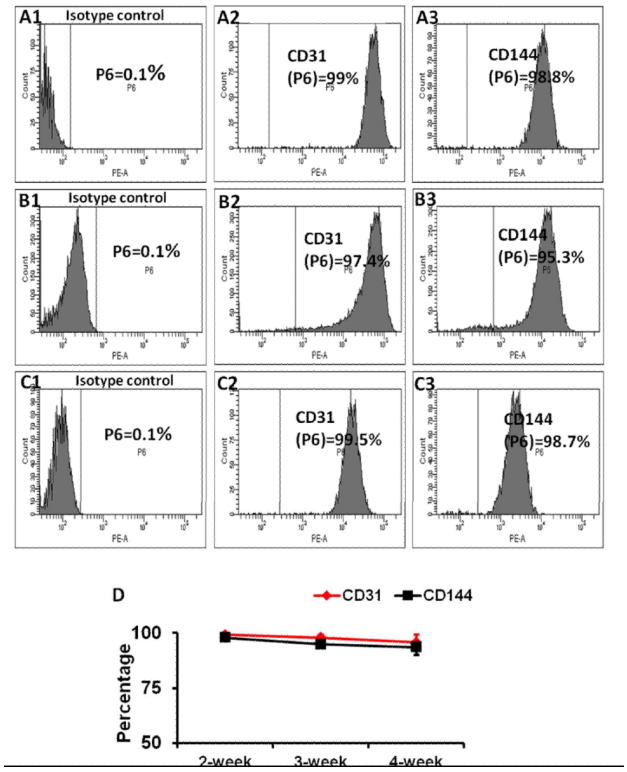

Figure 3. Differentiated hiPSC-ECs maintained EC characteristics for at least 4 weeks in vitro

Differentiated hiPSC-ECs were purified to >95% CD31+ cells via flow cytometry, and maintained in medium supplemented with VEGF and SB431542 for 14 days **(A1-A3)**, 21 days **(B1-B3)**, and 28 days **(C1-C3)**. The proportion of cells that expressed CD31 **(A2, B2, C2)** or CD144 **(A3, B3, C3)** were compared with isotype controls **(A1, B1, and C1)** and **(D)** presented as a function of time after purification.

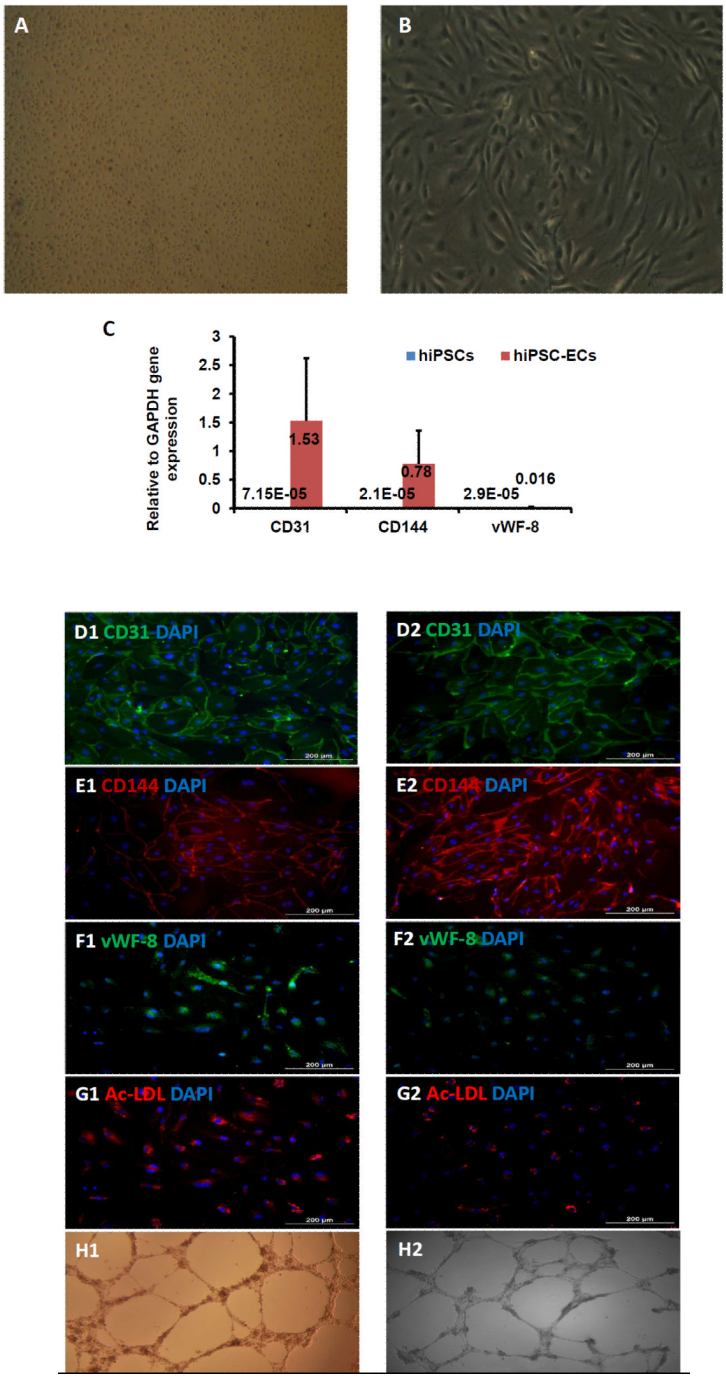

Figure 4. Characterization of differentiated hiPSC-ECs

The morphology of the differentiated hiPSC-ECs was evaluated via images obtained at **(A)** 25X or **(B)** 100X magnification. **(C)** The gene expression levels of CD31, CD144, and vWF-8 mRNA were normalized to GAPDH, and presented as fold changes. Protein expression of CD31, CD144, and vWF-8 at week-1 **(D1, E1, and F1)** and week-4 **(D2, E2, and F2)** after isolation were evaluated via immunofluorescence; nuclei were counterstained with DAPI. The biological function of hiPSC-ECs was evaluated via Dil-ac-LDL uptake and

the formation of tube-like structures on Matrigel at week-1 **(G1 and H1)** and week-4 **(G2 and H2)** after isolation; (Bar=200 μm, Panel E: magnification=200x).